Proceedings of the 20th International Conference on Soil Mechanics and Geotechnical Engineering– Rahman and Jaksa (Eds)

Behavior of closely spaced back-to-back MSE walls considering compaction and surcharge loads at ultimate limit state

Comportement des murs MSE étroitement espacés dos à dos en tenant compte du compactage et des charges supplémentaires à l'état limite ultime.

Dr. Umashankar Balunaini
Professor, Civil Engineering, IIT Hyderabad, India, buma@ce.iith.ac.in

Reddy Sridhar K
Former MTech student, Civil Engineering, IIT Hyderabad, India

Dr. Sasanka Mouli S
Assistant Professor, Civil Engineering, VNR VJIET, India

ABSTRACT: Back-to-back Mechanically Stabilized Earth (BBMSE) walls are common in narrow highway and railway bridge abutments. Federal Highway Administration (FHWA) publication "Design and Construction of Mechanically Stabilized Earth Walls and Reinforced Soil Slopes" covers the design of BBMSE walls, albeit briefly, highlighting the two extreme cases to obtain the modified lateral pressures at the end of the reinforced zone to perform the external stability check of the BBMSE walls. The distance between back-to-back walls is an important parameter to estimate the lateral pressures on BBMSE walls. In the present study, the numerical model of BBMSE walls with unconnected and connected reinforcements were developed considering compaction and surcharge loads. The complex interaction of slip surfaces formed in BBMSE walls at the ultimate limit state for varying distances between the walls were analyzed using a numerical method based on "Fast Lagrangian Analysis of Continua (FLAC, Version 8.00)". The influence of the compaction and surcharge loading on the mobilized lateral pressures and reinforcement tensile profiles was studied. The modified lateral pressure coefficients were proposed.

RÉSUMÉ : Les murs dos à dos en terre stabilisée mécaniquement (BBMSE) sont courants dans les culées étroites des ponts routiers et ferroviaires. La publication de la Federal Highway Administration (FHWA) « Design and Construction of Mechanically Stabilized Earth Walls and Reinforced Soil Slopes » couvre la conception des murs BBMSE, bien que brièvement, en soulignant les deux cas extrêmes pour obtenir les pressions latérales modifiées à la fin de la zone renforcée pour effectuer le contrôle de stabilité externe des murs BBMSE. La distance entre les murs dos à dos est un paramètre important pour estimer les pressions latérales sur les murs BBMSE. Dans la présente étude, le modèle numérique des murs BBMSE avec des armatures non connectées et connectées a été développé en tenant compte des charges de compactage et de surcharge. L'interaction complexe des surfaces de glissement formées dans les parois du BBMSE à l'état limite ultime pour des distances variables entre les parois a été analysée à l'aide d'une méthode numérique basée sur « Fast Lagrangian Analysis of Continua (FLAC, Version 8.00) ». L'influence de la charge de compactage et de surcharge sur les pressions latérales mobilisées et les profils de traction des renforts a été étudiée. Les coefficients de pression latérale modifiés ont été proposés.

KEYWORDS: back-to-back walls, interaction, compaction, surcharge load, ultimate limit state

1 INTRODUCTION

Back-to-back Mechanically Stabilized Earth (BBMSE) walls are extensively used for railroad bridge embankments, highway bridge approach embankments, tsunami barriers in coastal areas, etc. "Federal Highway Administration (FHWA)" (Berg et al. 2009) provides guidelines for single MSE walls. The guidelines also briefly discuss the design of BBMSE walls. The lateral pressures on these walls depend on the distance between the back-to-back walls. Two configurations were highlighted to estimate the modified lateral pressures for external stability calculations, namely, (1) the walls are far from each other, i.e., the clear distance between the ends of reinforced zones are greater than H times tan(45-ϕ/2); the walls in this case can be designed as independent single MSE walls, and (2) the walls are close to each other with the reinforcements overlapping by more than 0.3 times H; the lateral pressures in this case are considered as zero. For any configuration in between these two extreme cases (Fig. 1), the lateral pressures on the reinforced zone are proposed to be linearly interpolated in between the full active and zero thrust conditions.

Many numerical modelling studies based on Finite Element Method (FEM) or Finite Difference Method (FDM) are available in the literature. Mirmoradi and Ehrlich 2015; Huang et al. 2010; Hatami and Bathurst 2005; Ling and Leshchinsky 2003 are some of the numerical studies available on single MSE walls. While Sravanam et al. 2019, 2020; Benmebarek and Djabri 2017; Benmebarek et al. 2016; Han and Leshchinsky 2010 have conducted numerical studies on BBMSE walls.

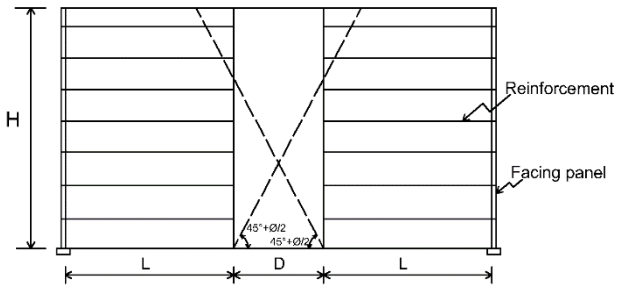

Figure 1. Interaction of slip surfaces in BBMSE walls

Sravanam et al. 2019 developed a robust back-to-back walls model using "Fast Lagrangian Analysis of Continua (FLAC)". The model was analysed under working loads considering compaction stresses and surcharge loads. Design charts for lateral pressures and reinforcement tensile forces were proposed. Parametric study for various reinforcement stiffness values and *W/H* ratios were analysed. Sravanam et al. 2020 analysed the behaviour of BBMSE walls at working stresses for connected and unconnected reinforcement cases. Tensile forces in the reinforcement and shear strain contours were studied in both extensible and inextensible reinforcements.

The present study was aimed on understanding the complex interaction behavior of BBMSE walls under compaction and surcharge stresses at ultimate limit state condition. *W/H* ratio was varied from 1.4 to 2.0 for a given reinforcement stiffness of J = 500 kN/m. The study analyses the interaction of slip surfaces of the BBMSE walls and its influence on the lateral pressures behind the reinforced zone. The present study was limited to studying the critical slip surfaces confined to reinforced zones.

2 MODEL DESCRIPTION

FLAC Version 8.00 (Itasca 2015) was used to simulate the numerical model of BBMSE walls. Segmental facing panels and backfill were modelled using continuum zones. Reinforcements were modelled using cable elements. Plane-strain condition was adopted and staged construction technique was incorporated to model the realistic construction procedure at the site.

Mesh size of 0.1 m*0.1 m was considered based on mesh convergence studies. The model was built in lifts of 0.725m. Compaction stresses (equal to 8 kPa) were applied on each lift and removed prior to proceeding to the next lift. A surcharge loading of 30 kPa was applied on the top of the fill after the construction of entire wall. The condition of propping of the facing panel was simulated by constraining horizontal movement of the facing panels till the end of construction. The ultimate limit state condition was simulated by rotating the entire walls outwards about their toes after construction of entire walls. Table 1 gives the geometry details of the BBMSE walls. Table 2 gives the backfill properties used in the FLAC model. Figure 2 shows the numerical models developed in FLAC for unconnected and connected BBMSE walls.

Table 1. Specifications of the walls considered in the study

Parameter	Value
Height of wall, H, in m	8
Vertical spacing between the reinforcement, S_v, in m	0.725
RCC segmental panel height, in m	0.725 m
Distance between the walls, W, in m	11.3, 13.6 and 16
W/H ratios	1.4, 1.7 and 2.0

Mohr-Coulomb model was used to simulate the fill materials. A non-linear stress-dependent stiffness model (Duncan et al. 1980) was used to consider the dependence of the deformation modulus of backfill on confining stress (Equations 1 & 2). Table 3 gives the values of the constants adopted in the hyperbolic equation. A detailed explanation of the upgradation procedure was given in Sravanam et al. 2019. A similar procedure was adopted in the present study. However, a simple linear elastic model was used to simulate the segmental facing panels.

$$E_t = \left[1 - \frac{R_f(1-sin\emptyset)(\sigma_1 - \sigma_3)}{2ccos\emptyset + 2\sigma_3 sin\emptyset}\right]^2 K_e P_a \left(\frac{\sigma_3}{p_a}\right)^n \quad (1)$$

$$B = K_b P_a (\sigma_3/p_a)^m \quad (2)$$

where, R_f = failure ratio; $\emptyset$ = angle of shearing resistance of backfill; c = cohesion of the backfill; σ_1 = major principal stress; σ_3 = minor principal stress; K_e = elastic modulus number; P_a = atmospheric pressure; n = elastic modulus exponent; K_b = bulk modulus number; and m = bulk modulus exponent.

Table 2. Backfill properties used for modelling in FLAC (Sravanam et al. 2020)

Property	Reinforced and retained backfill	Concrete Panel
Constitutive model	Mohr-Coulomb	Elastic
Angle of shearing resistance, $\emptyset$, degrees	34	
Density, ρ, kg/m^3	2,002	2,446
Initial Elastic Modulus, E, MPa	50	3.19e4
Poisson's ratio, μ	0.25	0.15

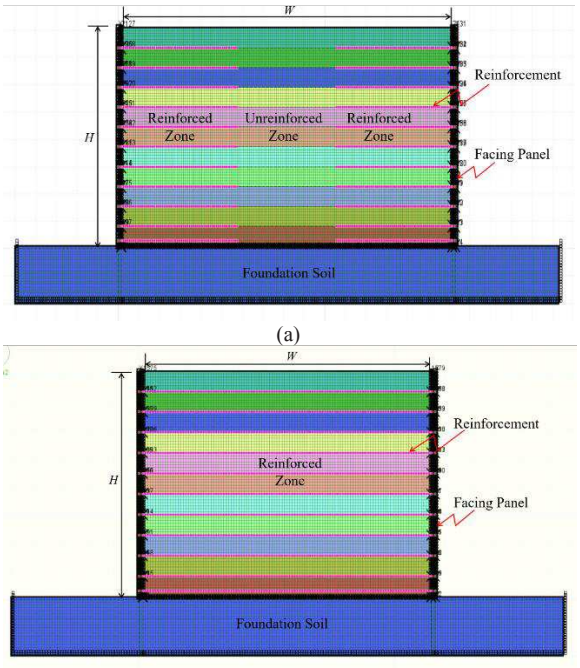

Figure 2. Numerical model of BBMSE walls with (a) unconnected reinforcement, and (b) connected reinforcement

The length of the reinforced zone (L) was considered as 0.7*H which was the minimum length as per FHWA guidelines. In FLAC, the interface between the reinforcement and backfill was simulated as inbuilt grout properties defined by bond stiffness and bond friction angle. Table 4 shows reinforcement properties used in the simulation.

Table 3. Hyperbolic stiffness model parameters of the backfill (Sravanam et al. 2020)

Input parameters used in the equation	Value
Failure ratio, R_f	0.86
Elastic modulus number, K_e	1150
Bulk modulus number, K_b	575
Elastic modulus exponent, n	0.5
Bulk modulus exponent, m	0.5

Table 4. Reinforcement properties used for modelling in FLAC (Sravanam et al. 2020)

Property	Value
Area, m^2	0.002
Axial Stiffness, J, kN/m	500
Bond Stiffness, N/m/m	2.3077e7
Friction Angle (degrees)	35

The foundation soil was assumed to be rigid so that the base failure condition was avoided. The bottom of the foundation soil was fixed in both the horizontal and vertical directions. The toe of walls was fixed in both horizontal and vertical directions and only rotation of walls about the toes was allowed. Interfaces were provided between the backfill and facing panels, between the facing panels and between the backfill and foundation soil in order to simulate the interaction between two different materials or joints (Table 5).

Table 5. Interface properties used for modelling in FLAC (Sravanam et al. 2020)

Property	Backfill and facing panel	Backfill and Foundation	Panel and Panel
Normal Stiffness, K_n, Pa/m	1.19e10	1.095e8	1.095e11
Shear Stiffness, K_s, Pa/m	2.31e7	1e7	1e10
Friction angle, δ, *degrees*	28	55	55
Cohesion, c, kPa	-	20	200

3 VALIDATION OF THE MODEL

The BBMSE wall model of the present study was validated with that of Han and Leshchinsky 2010. In Han and Leshchinsky 2010, the height of the walls was considered as 6 m with segmental panels each of 0.2m high. The length of the reinforcement was taken as 4.2 m (i.e., 0.7 times the height of the walls). The vertical spacing between the reinforcement layers was taken as 0.6 m. The ultimate limit state in the model was achieved by providing a weak interface zone of the toe of the walls.

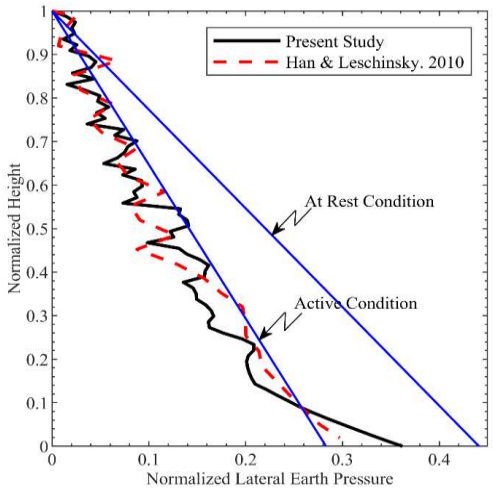

Figure 3. Comparison of lateral earth pressures at the end of reinforced zone from the present study with Han and Leshchinsky, 2010 corresponding to $W/H = 2.0$

The reinforcement stiffness was assumed to be 500kN/m. The limit state in the present study was simulated by rotating the facing about the toe. The normalized lateral pressures behind the reinforced zone from the present study was compared with those from Han and Leshchinsky 2010. Figure 3 shows the comparison of lateral earth pressures at the end of the reinforced zone with Han and Leshchinsky 2010, corresponding to $J = 500$ kN/m for W/H=2.0. The lateral pressures behind the reinforced zone from the present study compared very well with those of Han and Leshchinsky 2010. The overall percentage deviation between the lateral pressure distributions was less than 5%.

4 RESULTS AND DISCUSSIONS

4.1 *Unconnected reinforcement*

In order to attain the ultimate limit-state condition, the facing panels of both the walls were rotated outwards simultaneously about their toes. The panels were rotated till the lateral pressures on the wall converged to a constant value signifying that the limit state had been reached for that particular value of rotation. The rotations of about 5-6% of the height of the wall was imparted to reach the ultimate limit state condition. At this state, the critical slip surfaces were found to have been developed, and the mobilized lateral pressures were obtained and their variation with the height of the wall was studied.

4.1.1 *Critical slip surfaces for various W/H*

Figure 4 shows the maximum shear strain contours for various W/H ratios corresponding to reinforcement stiffness, J, equal to 500 kN/m. In the figure, the locus of the maximum shear strains was plotted with the black line. It was observed that the interaction between the slip surfaces of the walls reduces with the increase in the W/H ratio. The interaction was maximum for W/H=1.4, while minimal interaction was noticed for W/H=2.0. It was also observed that for W/H=1.7 and W/H=2.0, the shearing strains were high even at the junction of reinforced and unreinforced zone.

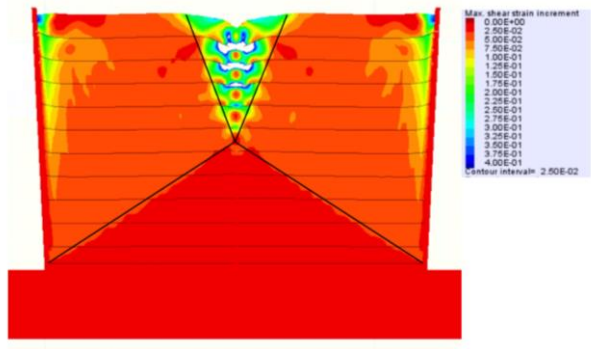

(a)

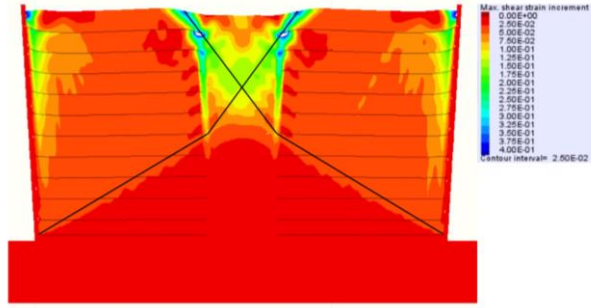

(b)

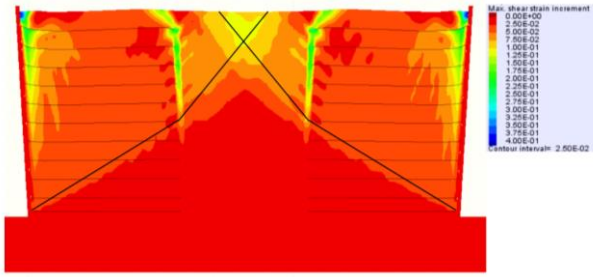

(c)

Figure 4. The maximum shear strain increment contours corresponding to reinforcement stiffness, *J*, equal to 500 kN/m for (a) *W/H* = 1.4, (b) *W/H* = 1.7, and (c) *W/H* = 2.0

4.1.2 *Lateral earth pressures behind the reinforced zone*

Figure 5 show the lateral earth pressure distributions behind the reinforced zone for various *W/H* ratios. The lateral pressures at the end of reinforced zone were a function of *W/H* ratio in BBMSE walls (Berg et al. 2009). The lateral pressures decrease with decrease in the *W/H* ratio. The lateral pressures developed were found to be less than the active condition (theoretical Coulomb's active earth pressure).

The interference of the critical slip surfaces of both the walls tend to reduce the lateral pressures behind the reinforced zone. In addition to the interaction of slip surfaces, the reduction in the lateral pressures behind the reinforced zone can also be attributed to the arching effect. The arching phenomenon in BBMSE walls was well explained in Sravanam et al. 2019.

4.1.3 *Modified lateral pressure coefficient, $K_{a,mod}$*

The resultant coefficients of lateral pressures were calculated for various *W/H* ratios. It was obtained by dividing the total lateral force with that of overall vertical load (i.e., $(0.5x\gamma xH^2)$ + *(Surcharge stress)*H*).

Table 6 gives the modified lateral pressure coefficients, $K_{a,mod}$, corresponding to various *W/H* ratios. It was observed that for the case with *W/H*=1.4 and *J*=500 kN/m, the modified lateral pressure coefficients, $K_{a,mod}$ had reduced by about 35% reduction in BBMSE walls from that of Coulomb's active condition. It can be inferred that $K_{a,mod}$ decreases with decrease in *W/H* ratio.

Figure 6 shows the comparison of $K_{a,mod}$ values corresponding to various *W/H* ratios. The modified lateral pressure coefficients, $K_{a,mod}$, thus calculated in the present study were much higher than those values recommended in FHWA manual. The $K_{a,mod}$ value for *W/H* =1.4 was about 95% higher than that of FHWA recommended value. However, the difference between these two values had reduced to zero as the *W/H* value increases. Hence, FHWA guidelines underestimate the modified total lateral force acting on the reinforced zone for the low *W/H* ratios (*W/H*<2.0). The variation of $K_{a,mod}$ was not linear with *W/H* ratio. However, FHWA had recommended to consider linear variation of K_a with *W/H* ratio.

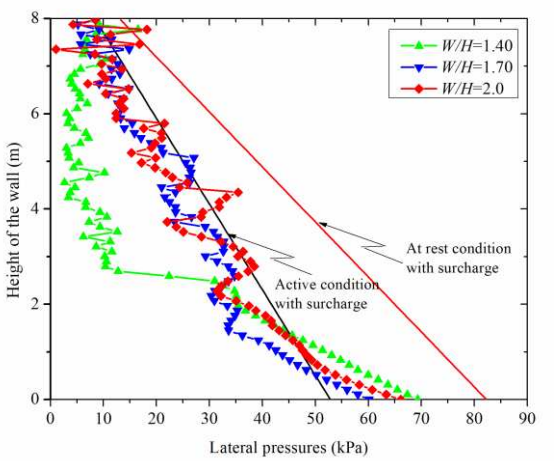

Figure 5. Comparison of lateral earth pressure distribution with the height of the wall for different *W/H* ratios

Table 6. $K_{a,mod}$ values for different *W/H*

W/H	Resultant Lateral force behind reinforced zone, F_r(kN/m)	$K_{a,mod}$= F_r/(0.5*γ *H^2 + Surcharge stress**H*)	$K_{a,mod}$ as per FHWA
	J = 500 kN/m	*J* = 500 kN/m	
1.1		0.000	0.000
1.4	161	0.186	0.094
1.7	213	0.245	0.189
2	229	0.263	0.283

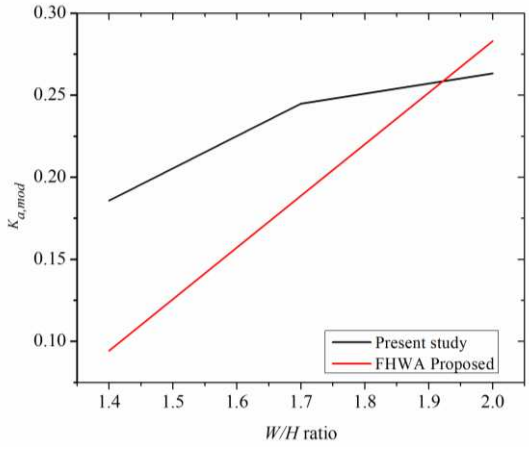

Figure 6. $K_{a,mod}$ *vs. W/H*

4.2 *Connected reinforcement*

The model was also analysed for the connected walls case. In connected walls, the reinforcement of both the walls were connected in the middle. In order to reach the ultimate limit-state condition, the facing panels of both the walls were rotated outwards simultaneously about their toes similar to that of unconnected walls case. The panels were rotated till the lateral pressures in the walls converge to a constant value. The walls were rotated by 0.2-0.5% of its height in order to reach the limit state.

4.2.1 *Formation of critical slip surface*

Figure 7 shows the maximum shear strain contours in connected walls. The critical slip surfaces were also marked in the figure. Significant difference was observed between the critical slip surfaces formed in the connected and unconnected walls. Even for relatively small displacements of the facing panels of the order of 0.5%, high shear strains were reflected only at the facing of the walls. This implies that the backfill near the wall facing could reach limit state in this region. However, the lateral displacements in the interior points of the walls were much less.

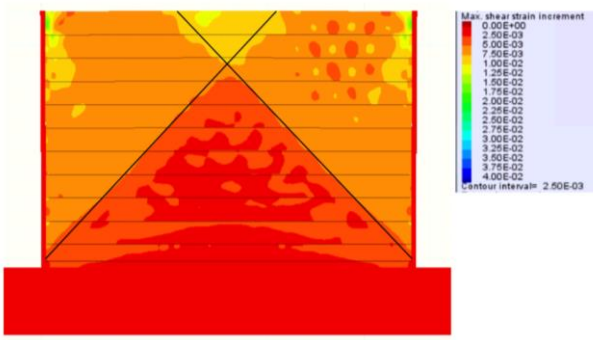

Figure 7. The maximum shear strain increment contours corresponding to reinforcement stiffness, J , equal to 500 kN/m

4.2.2 *Lateral earth pressures behind the reinforced zone*

Figure 8 shows the lateral pressure distribution at the facing. It was observed that lateral pressure distribution at the facing was almost equal to the Coulomb's active earth pressure distribution. The sharp increase in lateral pressures at the bottom of the wall was due to the boundary conditions applied at the toe of the wall, i.e., the lateral displacements were restrained at the toe of the walls.

FHWA guidelines discuss very little about the connected back-to-back walls. It recommends on adopting at-rest condition (K_o) for the design of connected walls. However, it is observed that the lateral pressures were much less than those of at-rest condition. Even at the working stresses, the lateral pressures in connected walls were not higher than those of the active condition (Sravanam et al. 2020).

4.3 *Comparison of maximum tensile force profiles for unconnected and connected walls*

Figure 9 shows the maximum tensile force profiles along the height of the wall in both connected and unconnected walls. In the present study, propping to the wall facing was applied throughout the construction phase of the wall and then it was allowed to rotate about the respective toes of the walls. Hence, the location of the maximum tensile forces in each reinforcement occurred at the reinforcement connection with the facing. As the ultimate limit-state condition was applied by rotating about the toe, the lateral displacement induced in the wall increases along the height of the wall (maximum at the top of the wall). Hence, the maximum tensile force in each reinforcement also increases with height of the wall in the unconnected walls. The maximum tensile profiles were much higher in the unconnected walls than those of connected walls. This was because the tensile forces were also the function of lateral displacements. The induced lateral displacements in the unconnected walls were much higher than those of the connected walls.

However, it was observed that the maximum tensile force profiles in connected walls was almost constant along the height of the wall. This is because of the reinforcements being connected between the walls. The tensile forces mobilized in the reinforcements were evenly distributed over the height of the wall.

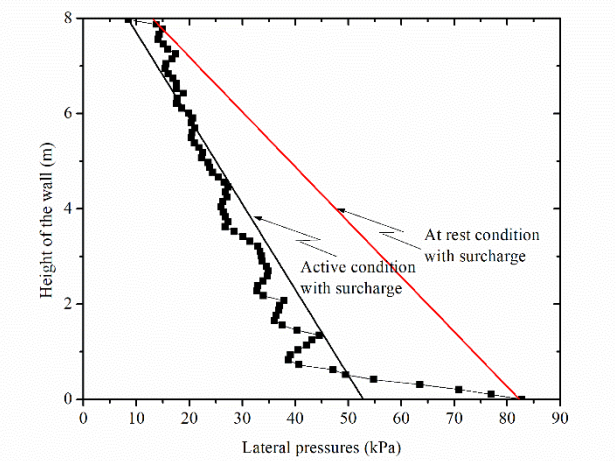

Figure 8. Lateral earth pressure distribution at the facing with respect to height of the wall

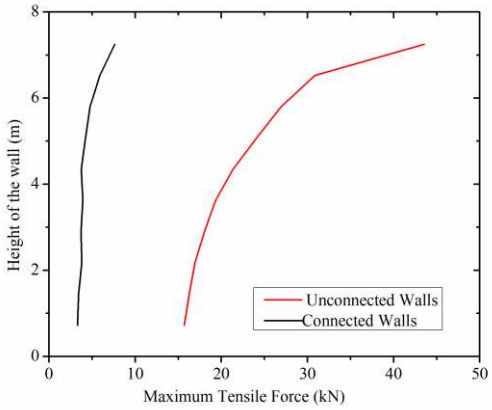

Figure 9. Maximum tensile force *vs.* height of the wall for unconnected and connected walls

5 CONCLUSIONS

The study focussed on analysing the interaction of critical slip surfaces of BBMSE walls and the modified lateral earth pressures behind the reinforced zone. The main conclusions of this study are as follows.

- In BBMSE walls, the interaction between slip surfaces decreased with increase in *W/H* ratio.
- The interaction of slip surfaces and the arching effect had led to the reduction of lateral pressures for walls with low *W/H* ratio. However, in the walls with high *W/H* ratio, the lateral pressures tend towards the Coulomb's active pressures.
- The coefficient of lateral earth pressure at the end of reinforced zone $K_{a,mod}$ was much higher than the value that is proposed by FHWA. The variation of $K_{a,mod}$ with

W/H ratio was not linear, as suggested to be considered in FHWA guidelines.

- In connected BBMSE walls, the lateral pressures at the facing were almost equal to Coulomb's active pressure.
- The maximum tensile force profiles in the reinforcements were almost constant in the connected walls. The maximum tensile profiles in the connected walls were much lower than those of unconnected walls.

6 REFERENCES

Benmebarek, S., Attallaoui, S., and Benmebarek, N. (2016). "Interaction analysis of back-to-back mechanically stabilized earth walls." Journal of Rock Mechanics and Geotechnical Engineering, 8(5), 697–702.

Benmebarek, S., and Djabri, M. (2017a). "FEM to investigate the effect of overlapping-reinforcement on the performance of back-to-back embankment bridge approaches under self-weight." Transportation Geotechnics, Elsevier Ltd, 11, 17–26.

Benmebarek, S., and Djabri, M. (2017b). "FE analysis of back-to-back Mechanically Stabilized Earth walls under cyclic harmonic loading." Indian Geotechnical Journal, Springer India, 48(3), 498–509.

Berg, R., Christopher, B., and Samtani, N. (2009). Design and construction of mechanically stabilized earth walls and reinforced soil slopes–Volume I. FHWA-NHI-10-024, Federal High Way Administration (FHWA), Washington, D.C.

Djabri, M., and Benmebarek, S. (2016). "FEM analysis of back-to-back geosynthetic-reinforced soil retaining walls." International Journal of Geosynthetics and Ground Engineering, Springer International Publishing, 2(3), 26.

Duncan, J. M., Byrne, P., Wong, K. S., and Mabry, P. (1980). Strength, stress-strain and bulk modulus parameters for finite element analysis of stress and movements in soil masses. Berkley, University of California, Berkley.

Han, J., and Leshchinsky, D. (2010). "Analysis of back-to-back mechanically stabilized earth walls." Geotextiles and Geomembranes, 28(3), 262–267.

Hatami, K., and Bathurst, R. J. (2005). "Development and verification of a numerical model for the analysis of geosynthetic-reinforced soil segmental walls under working stress conditions." Canadian Geotechnical Journal, 42(4), 1066–1085.

Huang, B., Bathurst, R. J., Hatami, K., and Allen, T. M. (2010). "Influence of toe restraint on reinforced soil segmental walls." Canadian Geotechnical Journal, 47(8), 885–904.

Itasca. (2015). FLAC-Fast Lagragian Analysis of Continua Version 8.00 User's Guide. Itasca Consulting Group Inc., Minnepolis, Minn.

Ling, H. I., and Leshchinsky, D. (2003). "Finite element parametric study of the behavior of segmental block reinforced-soil retaining walls." Geosynthetics International, 10(3), 77–94.

Madabhushi, S. S. C. (2018). "Multi-Hazard analysis of Dual Row Retaining Walls." Ph. D. Dissertation, University of Cambridge.

Mirmoradi, S. H., and Ehrlich, M. (2015). "Modeling of the compaction-induced stress on reinforced soil walls." Geotextiles and Geomembranes, 43(1), 82–88.

Rohith, M., Mouli, S., and Balunaini, U. (2018). "Interference of two closely-spaced footings on finite sand layer." Geotechnical Engineering journal of the SEAGS and AGSSEA, 49(1), 128–135.

Sravanam, S. M., Balunaini, U., and Madhav, M. R. (2019). "Behavior and Design of Back-to-Back Walls Considering Compaction and Surcharge Loads." International Journal of Geosynthetics and Ground Engineering, Springer International Publishing, 5(4), 1–17.

Sravanam, S. M., Balunaini, U., and Madhira, R. M. (2020). "Behavior of Connected and Unconnected Back-to-Back Walls for Bridge Approaches." International Journal of Geomechanics, 20(7), 1–10.